Wheel Forces Estimation via Adaptive Sub-Optimal Second Order Sliding Mode Observers

Conference Paper · October 2017

3 authors, including:

Enrico Regolin
University of Pavia
5 PUBLICATIONS **0** CITATIONS

SEE PROFILE

Wheel Forces Estimation via Adaptive Sub-Optimal Second Order Sliding Mode Observers

Enrico Regolin, Massimo Zambelli and Antonella Ferrara
Dipartimento di Ingegneria Industriale e dell'Informazione
University of Pavia, via Ferrata 5, 27100 Pavia, Italy
(e-mail: enrico.regolin@unipv.it, massimo.zambelli01@universitadipavia.it, a.ferrara@unipv.it)

***Abstract*—In this work a system for the estimation of the forces (both longitudinal and lateral) exerted between the tires and the road is presented. Starting from two of the most commonly used descriptions of the vehicle dynamics, the single-corner and the single-track models, a system composed of Sub-Optimal Second Order Sliding Mode observers in a cascade structure plus an adaptive element is developed and verified to be effective in conditions in which the effect of the weight transfer can be neglected. One notable property of this approach is that only standard sensors, which are present in most of the stock cars, are exploited. The practical implementation is done using a switched/time-based adaptation law for the gains of the observers, in order to be able to track the quantities in a wide range of conditions while keeping the chattering low. Simulation results are presented in IPG Car-Maker.**

***Index Terms*—Vehicle dynamics, Sliding mode control, Estimation, Automotive engineering**

I. Introduction

Active control systems in vehicles nowadays are of paramount importance, as they help to improve safety, efficiency and comfort. In order to have them working properly, accurate vehicle state information is needed. In particular, the knowledge about instantaneous tire-road forces can be exploited in many different ways (e.g. longitudinal and lateral dynamic stability control). Due to economic reasons, it is overly expensive for standard vehicles to equip sensors able to provide such measurements. It becomes then fundamental the contribution of online observers that only exploit standard sensors for accurate estimations.

In literature a lot of different approaches are presented, mainly devoted to the final aim of identifying the tire-road friction curve. One example can be found in [1], where an observer that uses the available measures of the wheels speed in combination with the LuGre model is used to identify changes in the road surface type. A different approach is adopted in [2], where the longitudinal and lateral tire forces are estimated using an Extended Kalman Filter (EKF) in combination with the vehicle single-track model, while using the Burckhardt parametrization for the tire-road friction forces. In [3] different methods for the estimation of the longitudinal tire forces are presented and exploited to identify the tire-road friction coefficient via recursive least squares. Ray estimates longitudinal and lateral forces using EKF in [4] or an Extended Kalman-Bucy filtering and Bayesian hypothesis selection [5]. While EKF is suitable for online estimation, it is sensible to inaccuracies in the friction model. An attempt to overcome this problem is done by introducing a proper correction generated by a Neural Network in [6]. Lateral forces are estimated in [7], using a four-wheels vehicle model and an EKF-based observer, and in [8] using a Super-Twisting Second Order Sliding Mode (ST-SOSM) based observer. Sliding mode is also used in [9], where its effectiveness in a real-time framework is analyzed. An experimental evaluation of a sliding mode observer is carried out in [10]. The application of longitudinal forces estimation for the online identification of the tire/road friction curve has been proposed by the authors in [11].

In the majority of the mentioned works only longitudinal or lateral dynamics are considered and some approximations are explicitly made (e.g. losses are neglected, steering angles are supposed small). In this work, an online adaptive Sub-optimal Second Order Sliding Mode (SSOSM) based observer is presented for the estimation of the instantaneous (both longitudinal and lateral) forces exerted between the tires and the road. In particular, it only exploits standard sensors and it is not based on a specific tire-road contact model. A combination of single-corner and single-track models is exploited: as a result, the observer is independent from the specific tire-road modelling and robust against road surface changes.

Work supported by EU Project ITEAM (project reference: 675999).

II. Vehicle Model

The purpose of the observer presented in this work is to provide an estimation for the longitudinal and lateral tire forces acting on the vehicle.

Throughout the discussion, continuous reference to the following symbols will be made:

$$F_{\mathrm{kl,ij}}, \quad k \in \{x,y\}; \quad l \in \{w,b\}; \quad i \in \{f,r\}; \quad j \in \{l,r\} \tag{1}$$

where k denotes a longitudinal or lateral force, l the reference frame (wheel or vehicle body), and the couple ij identifies the wheel (forward/rear, left/right). $\hat{F}$ represents the estimation of the considered force. For the modelling of the longitudinal forces it is possible to start from the first equation of the so-called single-corner model (see Fig. 1(a)), which considers the dynamics of a single wheel with respect to its own reference frame, as described e.g. in [12]. By introducing also an additional term T_{loss}, which takes into account all the losses (e.g. mechanical and aerodynamic friction), the following model is obtained

$$J_{\mathrm{w}}\dot{\omega} = T_{\mathrm{w}} - T_{\mathrm{loss}} - R_{\mathrm{e}}F_{\mathrm{xw}} \tag{2}$$

where J_{w}, ω, Re are the moment of inertia, the angular speed and the effective radius of the wheel, respectively, T_{w} is the torque acting on the wheel and F_{xw} is the traction/braking force (ij pedices are omitted, as for each wheel the same model is used).

In this work, we consider the total losses due to aerodynamic resistance and rolling resistance to be equally split between the 4 wheels. Although this assumption is not entirely correct in several situations, such as low speed cornering and hard

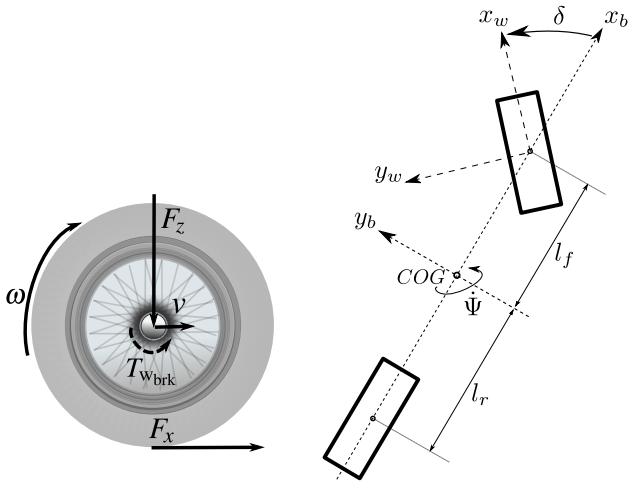

(a) Single Corner Model (b) Single Track Vehicle Model

Figure 1. Graphical representation of the models used

braking of selected wheels, it can be in general considered to be an improvement in the description of the longitudinal dynamics, compared to the case where T_{loss} is neglected.

For the lateral forces (referred to the vehicle reference frame), the modelling is made starting from the first part of the so-called single-track model (see e.g. [13]), schematically represented in Fig. 1(b), given by

$$\begin{cases} \ddot{\psi} = \frac{1}{J_z}(l_{\text{f}}F_{\text{yb,f}} - l_{\text{r}}F_{\text{yb,r}} + \frac{1}{2}b_{\text{f}}\Delta F_{\text{xb,f}} + \frac{1}{2}b_{\text{r}}\Delta F_{\text{xb,r}}) \\ F_{\text{yb,f}} = F_{\text{yb,fl}} + F_{\text{yb,fr}} \\ F_{\text{yb,r}} = F_{\text{yb,rl}} + F_{\text{yb,rr}} \\ \Delta F_{\text{xb,f}} = F_{\text{xb,fr}} - F_{\text{xb,fl}} \\ \Delta F_{\text{xb,r}} = F_{\text{xb,rr}} - F_{\text{xb,rl}} \end{cases} \tag{3}$$

where $\ddot{\psi}$ is the yaw rate, J_z is the vehicle total moment of inertia, l_{f}, l_{r} are the distances of the front and rear axles from the center of gravity, and b_{f}, b_{r} are the distances between the two wheels of the same (front or rear) axle. Since in this case the effects of the longitudinal forces on the overall yaw moment have to be taken into account as well, the two additional terms $\frac{1}{2}b_{\text{f}}\Delta F_{\text{xb,f}}$, $\frac{1}{2}b_{\text{r}}\Delta F_{\text{xb,r}}$ must be considered, which represent the moment generated by the differences in the longitudinal forces acting on the wheels of the same axle ($\Delta F_{\text{xb,k}}$).

III. Observers Description

In order to estimate the longitudinal forces $F_{\text{xw,ij}}$, an observer is used for each wheel, exploiting model (2). The knowledge of all the involved quantities, except for T_{loss} and the force itself, allows to develop a Sub-Optimal SOSM observer [14] which steers to zero the error

$$\sigma_{\text{x}} = \omega - \hat{\omega} \tag{4}$$

by controlling the system

$$J_{\text{w}}\dot{\hat{\omega}} = T_{\text{w}} - \hat{T}_{\text{loss}} - R_{\text{e}}u \tag{5}$$

where u is the observer input law. As a result, in analogy with [15], the estimated force is $\hat{F}_{\text{xw}} = u$.

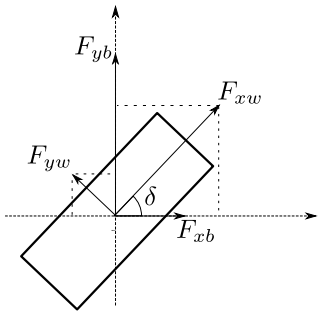

Figure 2. Front-left wheel forces representation

The loss term is estimated via the PI adaptive law

$$\hat{T}_{\text{loss}} = K_P \cdot \dot{e}_{\text{PI}} + K_I \cdot e_{\text{PI}}, \tag{6}$$

where $\hat{T}_{\text{loss}}$ is the estimate, K_P and K_I are the proportional and integral parameters of the PI, and the input error is given by

$$e_{\text{PI}} = ma_{\text{x}} - \sum_{\text{ij}}(\hat{F}_{\text{xb,ij}}), \tag{7}$$

in which m is the total mass of the vehicle and a_{x} is the longitudinal acceleration (with respect to the vehicle reference frame) measured by the vehicle accelerometer. As a result, the first term represents the total measured force, while the second one is the total estimated force. Since the estimation is based on model (2), in which the forces are referred to the wheels reference frames, a linear transformation has to be performed in order to guarantee consistency in presence of a non-null steering angle δ (see Fig. 2). Please note that δ, in a typical passenger vehicle has a limited range of possible values, so that one can assume

$$\cos(\delta) >> 0 \tag{8}$$

in all the considered situations. Moreover, in a common vehicle such transformation involves only the front wheels as they are affected by the steering angle. We consider the front-left wheel, since the same computations hold for the front-right one

$$\begin{cases} F_{\text{xb,fl}} = cos(\delta)F_{\text{xw,fl}} - sin(\delta)F_{\text{yw,fl}} \\ F_{\text{yb,fl}} = sin(\delta)F_{\text{xw,fl}} + cos(\delta)F_{\text{yw,fl}} \end{cases} \tag{9}$$

From the second equation in (9), $F_{\text{yw,fl}}$ can be derived and substituted into the first equation, obtaining

$$\begin{aligned} F_{\text{xb,fl}} &= \left(cos(\delta) + \frac{sin^2(\delta)}{cos(\delta)}\right)F_{\text{xw,fl}} - \frac{sin(\delta)}{cos(\delta)}F_{\text{yb,fl}} \\ &= \frac{1}{cos(\delta)}F_{\text{xw,fl}} - tan(\delta)F_{\text{yb,fl}} \end{aligned} \tag{10}$$

Repeating the same reasoning for the front-right wheel and considering the rear wheels as non-steering, the overall transformation required to obtain the terms in (7) turns out to be

$$\begin{cases} \hat{F}_{\text{xb,fl}} = \frac{1}{cos(\delta)}\hat{F}_{\text{xw,fl}} - tan(\delta)\hat{F}_{\text{yb,fl}} \\ \hat{F}_{\text{xb,fr}} = \frac{1}{cos(\delta)}\hat{F}_{\text{xw,fr}} - tan(\delta)\hat{F}_{\text{yb,fr}} \\ \hat{F}_{\text{xb,rl}} = \hat{F}_{\text{xw,rl}} \\ \hat{F}_{\text{xb,rr}} = \hat{F}_{\text{xw,rr}} \end{cases} \tag{11}$$

Regarding the lateral forces, only one observer is needed: making the assumption that two wheels attached to the same axle share the same lateral force (with respect to the vehicle reference frame), it is possible to exploit the single-track model described in (3). By merging it with the equation for the total lateral acceleration

$$ma_{\text{y}} = F_{\text{yb,f}} + F_{\text{yb,r}}, \tag{12}$$

in which it is assumed that the lateral acceleration a_{y} is available for measurement by means of an accelerometer, a SSOSM observer can be designed in order to steer to zero

the estimation error

$$\sigma_{\mathrm{y}} = \dot{\psi} - \hat{\dot{\psi}} \tag{13}$$

Then, the following system is obtained

$$\begin{cases} \dot{\hat{\psi}} = \frac{1}{J_z}[l_{\mathrm{f}} m a_{\mathrm{y}} - (l_{\mathrm{f}} + l_{\mathrm{r}})u + \frac{1}{2} b_{\mathrm{f}} \Delta \hat{F}_{\mathrm{xb,f}} + \frac{1}{2} b_{\mathrm{r}} \Delta \hat{F}_{\mathrm{xb,r}}] \\ \hat{F}_{\mathrm{yb,f}} = m a_{\mathrm{y}} - u \\ \Delta \hat{F}_{\mathrm{xb,f}} = \hat{F}_{\mathrm{xb,fr}} - \hat{F}_{\mathrm{xb,fl}} \\ \Delta \hat{F}_{\mathrm{xb,r}} = \hat{F}_{\mathrm{xb,rr}} - \hat{F}_{\mathrm{xb,rl}} \end{cases} \tag{14}$$

Due to the choices made, and with similar considerations as in the longitudinal case, it holds that the estimated force acting on the rear axle is $\hat{F}_{\mathrm{yb,r}} = u$. To estimate the lateral forces on each quarter-car, the force acting on each axis is equally splitted on the two corresponding wheels. This is a reasonable approximation if the difference in the normal forces acting on each of the two wheels is small enough. With this assumption, the following expression is valid

$$\begin{cases} \hat{F}_{\mathrm{yb,fl}} = \hat{F}_{\mathrm{yb,fr}} = \frac{1}{2}(m a_{\mathrm{y}} - \hat{F}_{\mathrm{yb,r}}) \\ \hat{F}_{\mathrm{yb,rl}} = \hat{F}_{\mathrm{yb,rr}} = \frac{1}{2}\hat{F}_{\mathrm{yb,r}} \end{cases} \tag{15}$$

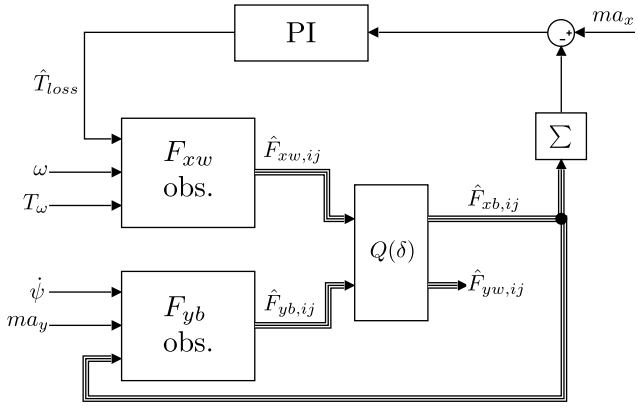

Figure 3. The complete observation scheme, where $Q(\delta)$ is the matrix representing the linear transformation from Equation (11)

By merging all the described parts, the complete scheme appears as in Fig. 3. In the next section the finite-time convergence of the whole system is analyzed.

IV. Convergence Analysis

In order to verify the convergence of the whole cascade system with adaptive law, the finite-time convergence of the two SSOSM observers is considered independently. In [14] the convergence of the SSOSM algorithm is proven, for a suitable choice of the observer gain K, under the hypothesis that the terms ϕ and D in the so-called auxiliary problem, i.e.

$$\begin{cases} \dot{\zeta}_1 = \zeta_2 \\ \dot{\zeta}_2 = \phi + D\dot{u} \end{cases} \tag{16}$$

satisfy the conditions

$$\begin{cases} |\phi| < \Phi \\ 0 < D_1 < D < D_2. \end{cases} \tag{17}$$

Note that, in the considered application, $\zeta_1 = \sigma_{\mathrm{k}}$, where k is defined as in (1). Under these hypothesis, the observer input law

$$\dot{u}(t) = -\alpha^* \cdot K \cdot \mathrm{sign}\left(\sigma_{\mathrm{k}}(t) - \frac{1}{2}\sigma_{\mathrm{k,MAX}}\right), \tag{18}$$

where $\sigma_{\mathrm{k,MAX}}$ is the value of σ_{k} at the last peak detection (i.e. when $\dot{\sigma}_{\mathrm{k}} = 0$), ensures that the sliding variable σ_{k} and its derivative $\dot{\sigma}_{\mathrm{k}}$ converge in finite time to the origin. In this context it can be assumed without loss of generality $\alpha^* = 1$, with the aim of reducing complexity. In the following it will be shown that conditions (17) are verified for the models (5) and (14) under the following reasonable assumptions:

- **a1)** All the physical quantities which affect the observers dynamics are bounded, with bounded first derivative;
- **a2)** The real behavior of the considered systems is fully captured by the used models, except for some terms (possibly nonlinear) which represent the unmodelled part and are bounded with bounded first derivative.

Then, the observers will be considered as a unique system featuring a PI logic, which is in charge of increasing the tracking precision of the observed quantities via the adaptive estimation of the loss term $\hat{T}_{\mathrm{loss}}$.

A. Convergence of the longitudinal forces estimation

In order to prove the convergence of the four observers for the longitudinal forces, it is sufficient to consider only one of them, as the same procedure can be adopted for all the others. Let us consider the term $\hat{T}_{\mathrm{loss}}$ as an exogenous disturbance with bounded first derivative. This is a reasonable assumption, as it is the output of a PI controller fed by the limited and continuous error e_{PI} defined in (7). Indeed,

$$\begin{aligned} e_{\mathrm{PI}} &= m a_{\mathrm{x}} - \sum_{\mathrm{ij}} (\hat{F}_{\mathrm{xb,ij}}) \\ &= m a_{\mathrm{x}} + \sum_{\mathrm{j}} [\frac{1}{\cos(\delta)} \int (K_{\mathrm{x}} \mathrm{sign}(\sigma_{\mathrm{x}} - \frac{\sigma_{\mathrm{x,MAX}}}{2})_{\mathrm{fj}}) + \\ &+ tan(\delta) \int (K_{\mathrm{y}} \mathrm{sign}(\sigma_{\mathrm{y}} - \frac{\sigma_{\mathrm{y,MAX}}}{2})_{\mathrm{fj}}) + \\ &+ \int (K_{\mathrm{x}} \mathrm{sign}(\sigma_{\mathrm{x}} - \frac{\sigma_{\mathrm{x,MAX}}}{2})_{\mathrm{rj}})] \end{aligned} \tag{19}$$

is limited, since m and a_{x} are physical quantities and the SSOSM observers have sufficiently high gains so that the sliding variables σ_{k} move towards the origin. Therefore, due to assumption a1) $m\dot{a}_{\mathrm{x}}$ is limited, and so is also $\dot{e}_{\mathrm{PI}}$. Let us also assume that the real dynamics of the wheel are described by model (2), plus a term U_{x} which represents the uncertainties affecting the system and satisfies assumptions a1) and a2), so that the new model considered is

$$\dot{\omega} = \frac{1}{J_{\mathrm{w}}}(T_{\mathrm{w}} - T_{\mathrm{loss}} - R_{\mathrm{e}} F_{\mathrm{w}}) + U_{\mathrm{x}} \tag{20}$$

The dynamic equation of the corresponding observer is presented in Equation (5). Hence, the second derivative of the chosen sliding variable (Equation (4)) is

$$\begin{aligned} \ddot{\sigma}_{\mathrm{x}} &= \ddot{\omega} - \ddot{\hat{\omega}} \\ &= \frac{1}{J_{\mathrm{w}}}(\dot{\hat{T}}_{\mathrm{loss}} - \dot{T}_{\mathrm{loss}} - R_{\mathrm{e}} \dot{F}_{\mathrm{xw}}) + \dot{U}_{\mathrm{x}} + \frac{R_{\mathrm{e}}}{J_{\mathrm{w}}}\dot{u} \\ &= \phi_{\mathrm{x}} + D_{\mathrm{x}}\dot{u} \end{aligned} \tag{21}$$

According to assumption a1) previously made, a bound Φ_{x} exists such that $|\phi_{\mathrm{x}}| \leq \Phi_{\mathrm{x}}$ and $D_{\mathrm{x}} = \frac{R_{\mathrm{e}}}{J_{\mathrm{w}}}$. Therefore, for a properly chosen gain K_{x}, the convergence is guaranteed ($\dot{\sigma}_{\mathrm{x}} = 0$), leading in finite time to

$$\hat{F}_{\mathrm{xw}} = u = F_{\mathrm{xw}} + \frac{1}{R_{\mathrm{e}}}(T_{\mathrm{loss}} - \hat{T}_{\mathrm{loss}}) + \frac{J_{\mathrm{w}}}{R_{\mathrm{e}}} U_{\mathrm{x}} \tag{22}$$

One can see from (22) how a necessary condition for the estimation of $\hat{F}_{\mathrm{xw}}$ is that the torque loss estimation error $\tilde{T}_{\mathrm{loss}} = T_{\mathrm{loss}} - \hat{T}_{\mathrm{loss}}$ is bounded. This will be proven in Subsection IV-C.

B. Convergence of the lateral forces estimation

In order to prove the convergence of the observer for the lateral forces acting on the wheels (referred to the vehicle

reference frame), it is sufficient to note that the estimation of the F_{xw} forces can be determined from the input of the SSOSM observers. Moreover, as noted in Section III, $\hat{\dot{F}}_{xw} = -K_x sign(\sigma_x - \frac{\sigma_{x,MAX}}{2})$ is always bounded. Assuming that the real dynamics of the yaw rate are described by Equation (3) plus an additional U_y term representing the uncertainties, the first equation of (3) becomes

$$\ddot{\psi} = \frac{1}{J_z}(l_f F_{yb,f} - l_r F_{yb,r} + \frac{1}{2} b_f \Delta F_{xb,f} + \frac{1}{2} b_r \Delta F_{xb,r}) + U_y \quad (23)$$

Since the observer used is the one described in Equation (14), the second derivative of the chosen sliding variable (13) is

$$\begin{aligned} \ddot{\sigma}_y &= \ddot{r} - \dot{\hat{r}} \\ &= \frac{1}{J_z}\left[\frac{b_f}{2}(\Delta \dot{F}_{xb,f} - \Delta \dot{\hat{F}}_{xb,f}) + \frac{b_r}{2}(\Delta \dot{F}_{xb,r} - \Delta \dot{\hat{F}}_{xb,r})\right] + \\ &- \frac{(l_f + l_r)}{J_z}\dot{F}_{y,r} + \dot{U}_y + \frac{(l_f + l_r)}{J_z}\dot{u} \\ &= \phi_y + D_y \dot{u} \end{aligned} \quad (24)$$

where $r = \dot{\psi}$. Similarly to the longitudinal case, thanks to assumption a1), one can say that a bound Φ_y exists such that $|\phi_y| \leq \Phi_y$ and $D_y = \frac{(l_f + l_r)}{J_z}$. Therefore, assuming a sufficiently high K_y is selected, the convergence is guaranteed ($\dot{\sigma}_y = 0$). If the same $\hat{T}_{loss}$ is considered for all the wheels (as it is the case), this leads in finite time to the following value for the estimation $\hat{F}_{yb,r} = u$:

$$\hat{F}_{yb,r} = F_{yb,r} + \xi \quad (25)$$

where

$$\begin{aligned} \xi = &\frac{J_w}{2R_e(l_f + l_r)}\left[\frac{1}{cos(\delta)} b_f (U_{x,fl} - U_{x,fr}) + \right. \\ &\left. - b_r (U_{x,rr} - U_{x,rl})\right] + \frac{J_z}{l_f + l_r} U_y \end{aligned} \quad (26)$$

Notice that the term ξ only depends on the uncertainties, and considering also the inequality (8), one can see how the steering angle does not introduce excessive error amplification. The convergence of the front axle force estimation comes as a consequence, based on the second Equation in (14).

C. Convergence of the torque loss estimation

Since the observers converge in finite time and the effects of T_{loss} are only present in the estimations of the F_{xw} forces, the estimated total longitudinal force can be considered as the output of a system fed only with time-varying disturbances and with $\hat{T}_{loss}$ as the control variable. Having defined $\hat{F}_{yb,f} := \hat{F}_{yb,fl} + \hat{F}_{yb,fr}$, one has:

$$\begin{aligned} \sum \hat{F}_{xb} &= \frac{1}{cos(\delta)}(\hat{F}_{xw,fl} + \hat{F}_{xw,fr}) - tan(\delta)\hat{F}_{yb,f} + \hat{F}_{xw,rl} + \hat{F}_{xw,rr} \\ &= \frac{1}{cos(\delta)}(F_{xw,fl} + F_{xw,fr} + \frac{2(T_{loss} - \hat{T}_{loss})}{R_e} + \\ &+ \frac{J_w}{R_e}(U_{x,fl} + U_{x,fr})) - tan(\delta)(ma_y - F_{yb,r} - \xi) + F_{xw,rl} + \\ &+ F_{xw,rr} + \frac{2(T_{loss} - \hat{T}_{loss})}{R_e} + \frac{J_w}{R_e}(U_{x,rl} + U_{x,rr}) \\ &= \sum F_{xb} + \kappa + \left(1 + \frac{1}{cos(\delta)}\right)\frac{2(T_{loss} - \hat{T}_{loss})}{R_e} \end{aligned} \quad (27)$$

where

$$\kappa = \frac{J_w}{R_e}\left(\frac{1}{cos(\delta)}(U_{x,fl} + U_{x,fr}) + U_{x,rl} + U_{x,rr}\right) + tan(\delta)\xi \quad (28)$$

When evaluating the estimation error for the total longitudinal force e_{F_x}, the uncertainty term c (respecting assumption a2)) is considered, in order to account for the measurement deviation. In this way, one obtains:

$$\begin{aligned} e_{F_x} &= \sum F_{xb} + c - \sum \hat{F}_{xb} \\ &= -\left(1 + \frac{1}{cos(\delta)}\right)\frac{2(T_{loss} - \hat{T}_{loss})}{R_e} - \kappa + c \end{aligned} \quad (29)$$

The error e_{F_x} vanishes asymptotically under the action of the PI controller (providing suitable proportional and integral parameters), leading to the following expression for the torque losses estimation:

$$\tilde{T}_{loss} = (c - \kappa)\frac{R_e cos(\delta)}{2(cos(\delta) + 1)} \quad (30)$$

One can see from Equations (26), (28) and (30) how the total estimation error $\tilde{T}_{loss}$ is also bounded, with bounded first derivative, as requested in Subsection IV-A for the convergence of the longitudinal force estimation.

V. Practical implementation and simulations

By exploiting results from [14] it is possible to compute a region in the (K_x, K_y) plane which leads to finite-time convergence for the two SSOSM observers. Moreover, from a theoretical viewpoint, it is needed to guarantee that the longitudinal forces observer converges faster than the one for the lateral forces, according to the so-called "control hierarchy" method illustrated in [16]. A detailed discussion of the convergence rates will be proposed in future works.

The gains which fall into the mentioned region are sufficient to guarantee the theoretical effectiveness of the proposed observation system. This holds in a large class of use cases (even non-standard, if a worst-case analysis is carried out), at the cost of increased gains. The control law is only used for estimation, so the common problems involving the actuators (e.g. mechanical wearing) do not arise. Nevertheless, the chattering is surely an effective problem if accurate results are needed. In a real implementation, usually the following holds:

- The geometrical values of the vehicle are well-known;
- The maximum rate of variation of the involved quantities can be studied, using the knowledge about the characteristics of sensors and actuators;
- The class of situations in which the observation has to be performed can be identified;
- A trade-off between accuracy and chattering can be achieved, considering the practical usage of the estimations.

Hence, suitable values for the gains could be tailored for the specific application. Possibly, they can happen to be far smaller than the ones theoretically determined making reference to the worst case. This might make the system unable to perform well in all the theoretical situations. In order to preserve convergence while avoiding the consequent chattering, an adaptive tuning of the gains could be introduced. In this paper the combined switched/time-based adaptation (STBA-SOSM) method is used [17]. An adaptive law is introduced for the determination of the gain of each observer. In particular, the instantaneous gain is given by

$$K(t) = K_s(t) + K_{tb}(t) \quad (31)$$

In (31) $K_s(t)$ is determined by a switched adaptation law, hereafter briefly outlined, referring the reader to [17] for the details. The $(\sigma_k, \dot{\sigma}_k)$ state-space is partitioned into a certain number of

regions $R_j, j=0,\ldots,l$ as, for example, in Fig. 5(a). The values of σ_k and $\dot{\sigma}_k$ determining each region have to be selected properly. To each region a specific gain K_j is associated, to be used when the current value of the pair $(\sigma_k, \dot{\sigma}_k)$ lies in the region.

The second term in (31), $K_{tb}(t)$, is a piece-wise constant term determined on the basis of the so-called "sliding mode indicator": the time is sliced in intervals of fixed length T and, at the end of each interval T_i, the number of zero-crossings $N_{sw,i}$ of the quantity $\sigma_k(t) - \frac{1}{2}\sigma_{k,MAX}$ is considered. Note that a high number of such crossings ($N_{sw,i} \geq N^*$, where N^* has to be properly chosen) is associated with the occurrence of the sliding mode behavior, revealing that the current gain is sufficiently high. The K_{tb} term can hence be reduced accordingly. On the contrary, a low number of crossings reveals the inability of the current gain to produce the sliding mode behavior, so it is must be increased. In particular, Algorithm 1 is used. In the algorithm

Algorithm 1 STBA Algorithm: Time Based Component

$$K_{tb}(t) = K_M^i, \quad t \in T_i \tag{32}$$

$$K_M^1 = 0 \tag{33}$$

$$K_M^{i+1} = \begin{cases} \max(K_M^i - \Lambda_1 T, -K_l) & \text{if} \quad N_{sw}(t) \geq N^* \\ \min(K_M^i + \Lambda_2 T, 0) & \text{if} \quad N_{sw}(t) < N^* \end{cases} \tag{34}$$

Λ_1 and Λ_2 are constants to be properly selected and K_l is the gain of the switched adaptation rule in the innermost region.

To verify the effectiveness of the presented system, two simulations are carried out in IPG Car-Maker: in the first one a steering maneuver is performed. The estimated forces are then compared with the actual ones, and the used STBA-SOSM parameters are presented as an example. To further verify the validity of the scheme also a purely longitudinal braking maneuver over two different road surfaces is simulated in IPG Car-Maker, using a known static Pacejka friction model. The forces obtained from the observation are used for an offline non-linear LS estimation of the curve parameters. The real and the estimated curves are then compared.

A. Steering maneuver

In this simulation the front axle is considered. The maneuver starts at the initial velocity of $40 km/h$ and the stability control is deactivated. The steering angle $\delta(t)$ changes with a sinusoid-like trajectory in the interval $2s-10s$. The results of the lateral force observation are presented in Fig. 4, for the front axle.

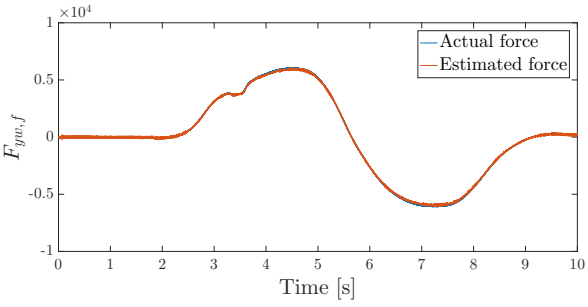

Figure 4. Lateral force estimation: front axle

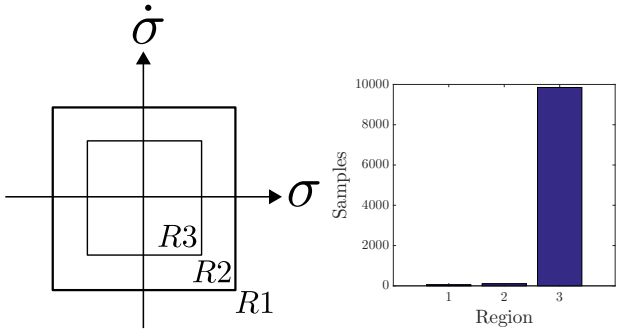

(a) Example of switching regions in the STBA algorithm

(b) Distribution of samples in the switching regions from the steering maneuver simulation

Figure 5. STBA algorithm representation

Table I
$K_{s,x}(t)$ SWITCHED LAW PARAMETERS

Region	Gain K_x	$\lvert\sigma_x\rvert$ Interval	$\lvert\dot{\sigma}_x\rvert$ Interval
1	200000	$20-\infty$	$50-\infty$
2	50000	$15-20$	$25-50$
3	25000	$2.5-15$	$10-25$
4	10000	$1-2.5$	$2.5-10$
5	2500	$0-1$	$0-2.5$

Table II
$K_{s,y}(t)$ SWITCHED LAW PARAMETERS

Region	Gain K_y	$\lvert\sigma_y\rvert$ Interval	$\lvert\dot{\sigma}_y\rvert$ Interval
1	1500	$10-\infty$	$25-\infty$
2	250	$2.5-10$	$5-25$
3	100	$0-2.5$	$0-5$

Table III
$K_{tb}(t)$ TIME-BASED ADAPTATION PARAMETERS

Observer	N^*	T	Λ_1	Λ_2
F_x	6	0.01	50000	25000
F_y	2	0.01	25000	12500

The parameters of the STBA-SOSM are reported in Table I for the longitudinal, and in Table II for the lateral forces. The time based law for the two observers uses the parameters reported in Table III.

As an indication of the general behavior of the observer, the number of time instants in which the pair $(\sigma_y, \dot{\sigma}_y)$ lies in each of the regions during the simulation is plotted in Fig. 5(b). Notice that Region 1 (the more external) is the only one in which it is necessary to have a sufficiently high gain in order to maintain the tracking ability. In the other regions, the gain has to be selected as small as possible in order to avoid excessive chattering while keeping $(\sigma_k, \dot{\sigma}_k)$ at least in the same region. In general, the more samples fall in internal regions (higher-numbered ones in this case), the more effective is the observation in terms of tracking precision and chattering avoidance.

B. Braking Maneuver

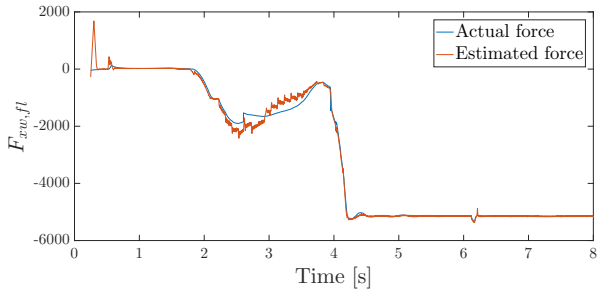

Figure 6. Longitudinal force estimation: front-left wheel

This simulation involves a purely longitudinal braking maneuver, performed in a straight road with three different surface types. The friction coefficients are computed via a static Pacejka friction model from known parameters. At the beginning a cruise phase is present, during which (at 1.44s) the first surface change occurs. Then, at 1.78s, a braking request is sent to the ABS controller, which acts in order to maintain an almost sinusoidal slip until the end of the simulation. At 2.67s the road surface changes again, and remains the same until 4.02s, when it returns to be the high-grip initial one. The lateral forces involved are negligible, so only the plot of the longitudinal forces is proposed. The robustness of the observer against the road surface changes can be appreciated in Fig. 6.

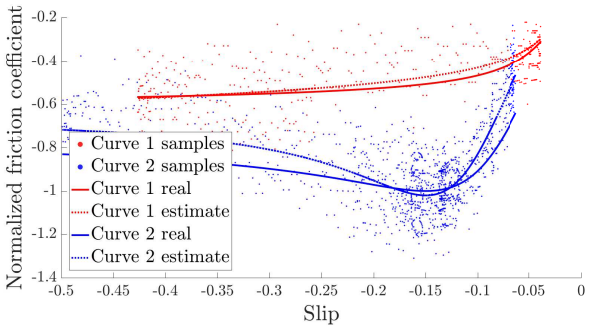

Figure 7. Longitudinal force identification: Tire/Road curve identification

By starting from the observations of the longitudinal force (rear-left tire) and the slip (which in practice can be easily obtained using a vehicle velocity observer such as the one in [18], an offline parameters estimation is performed. For the sake of clarity in the plot, only two different surfaces are considered: the samples are taken starting from 2.67s. The results, obtained using a nonlinear least squares method, are presented in Fig. 7.

VI. Conclusions

In this paper, an observer for the estimation of the longitudinal and lateral forces acting on a vehicle is presented. The observer is composed of the cascade of two Sub-optimal Second Order Sliding Mode observers, with switched/time-based adaptation of the observer gains, plus an adaptive feedback loop for the estimation of the longitudinal torque losses. The different bandwidths of the Sliding Mode observers are exploited, in order to prove the convergence of the observed quantities.

The proposed observer shows promising results in the presented simulations, which are performed in IPG Car-Maker.

The authors plan to provide formal proof of the different convergence rates of the Sliding Mode observers as a future development of this work. Next research may also include the extension of the longitudinal vehicle model to the cases where different torque losses for each wheel are estimated and the normal forces distribution is taken into account, as well as the experimental application of the algorithm on a test vehicle.

References

[1] C. Canudas-De-Wit and R. Horowitz, "Observers for tire/road contact friction using only wheel angular velocity information," *Proceedings of the 38th Conference on Decision & Control*, 1999.

[2] G. Baffet, A. Charara, and G. Dherbomez, "An observer of tire-road forces and friction for active security vehicle systems," *IEEE/ASME Transactions on Mechatronics*, vol. 12, no. 6, pp. 651–661, 12 2007.

[3] R. Rajamani, G. Phanomchoeng, D. Piyabongkarn, and J. Y. Lew, "Algorithms for real-time estimation of individual wheel tire-road friction coefficients," *IEEE/ASME Transactions on Mechatronics*, vol. 17, no. 6, pp. 1183–1195, Dec. 2012.

[4] L. R. Ray, "Nonlinear state and tire force estimation for advanced vehicle control," *IEEE Transactions on Control Systems Technology*, vol. 3, no. 1, pp. 117–124, 03 1995.

[5] ——, "Nonlinear tire force estimation and road friction identification: Simulation and experiments," *Automatica*, vol. 33, no. 10, pp. 1819–1833, 1997.

[6] J. Matuško, I. Petrović, and N. Perić, "Neural network based tire/road friction force estimation," *Engineering Applications of Artificial Intelligence*, vol. 21, no. 3, pp. 442–456, 2008.

[7] M. Doumiati, A. Victorino, A. Charara, and D. Lechner, "A method to estimate the lateral tire force and the sideslip angle of a vehicle: Experimental validation," *2010 American Control Conference*, 2010.

[8] R. Tafner, M. Reichhartinger, and M. Horn, "Estimation of tire parameters via second-order sliding mode observers with unknown inputs," in *13th IEEE Workshop on Variable Structure Systems*, 2014.

[9] H. Guo, H. Chen, and T. Song, "Tire-road forces estimation based on sliding mode observer," *Proceedings of the 2009 IEEE International Conference on Mechatronics and Automation*, 08 2009.

[10] G. Baffet, A. Charara, and D. Lechner, "Experimental evaluation of a sliding mode observer for tire-road forces and an extended kalman filter for vehicle sideslip angle," *Proceedings of the 46th IEEE Conference on Decision and Control*, 12 2007.

[11] E. Regolin and A. Ferrara, "Svm classification and kalman filter based estimation of the tire-road friction curve," in *Proceedings of the 20th World Congress of the International Federation of Automatic Control (IFAC)*, 2017.

[12] E. Regolin, G. P. Incremona, and A. Ferrara, *Sliding mode control of vehicle dynamics*. IET, London, 2017, ch. Longitudinal Vehicle Dynamics Control via Sliding Modes Generation, pp. 33–76.

[13] E. Regolin, D. Savitski, V. Ivanov, K. Augsburg, and A. Ferrara, *Sliding mode control of vehicle dynamics*. IET, London, 2017, ch. Lateral Vehicle Dynamics Control via Sliding Modes Generation, pp. 121–158.

[14] G. Bartolini, A. Ferrara, and E. Usai, "Chattering avoidance by second-order sliding mode control," *IEEE Transactions on Automatic Control*, vol. 43, no. 2, 02 1998.

[15] M. Tanelli, A. Ferrara, and P. Giani, "Combined vehicle velocity and tire-road friction estimation via sliding mode observers," in *Proc. IEEE International Conference on Control Applications*, Oct. 2012, pp. 130–135.

[16] R. A. DeCarlo, S. H. Zak, and G. P. Matthews, "Variable structure control of nonlinear multivariable systems: a tutorial," *Proceedings of the IEEE*, vol. 76, no. 3, pp. 212–232, 1988.

[17] A. Pisano, M. Tanelli, and A. Ferrara, "Combined switched/time-based adaptation in second order sliding mode control," *52nd IEEE Conference on Decision and Control*, 2013.

[18] M. Tanelli, L. Piroddi, and S. M. Savaresi, "Real-time identification of tire-road friction conditions," *IET Control Theory and Applications*, vol. 3, no. 7, pp. 891–906, Jul. 2009.